ARTICLE
Journal of Cellular Biochemistry 115:2175–2187 (2014)

Journal of Cellular Biochemistry

Progeny From Irradiated Colorectal Cancer Cells Acquire an EMT-*Like* Phenotype and Activate Wnt/β-Catenin Pathway

Lilian Gonçalves dos Reis Bastos,[1] Priscila Guimarães de Marcondes,[1] Julio Cesar Madureira de-Freitas-Junior,[1] Fernanda Leve,[2] André Luiz Mencalha,[3] Waldemir Fernandes de Souza,[1] Wallace Martins de Araujo,[1] Marcelo Neves Tanaka,[4] Eliana Saul Furquim Werneck Abdelhay,[5] and José Andrés Morgado-Díaz[1]*

[1]*Cellular Biology Program, Brazilian National Cancer Institute (INCA), 37André Cavalcanti Street, 5th Floor, Rio de Janeiro, RJ 20230-051, Brazil*

[2]*National Institute of Metrology, Quality and Technology (INMETRO), 50, Nossa senhora das Graças Avenue, Building 27, Xerém, Duque de Caxias, RJ 25250-020, Brazil*

[3]*Department of Biophysics and Biometry, Rio de Janeiro State University (UERJ), 87 Vinte e Oito de Setembro Avenue, 4th Floor, Rio de Janeiro, RJ 20551-030, Brazil*

[4]*Brazilian Center For Physics Research (CBPF), 150, Dr. Xavier Sigaud Street - Urca, Rio de Janeiro, RJ 22290-180, Brazil*

[5]*Bone Marrow Transplantation Unit, National Cancer Institute (INCA), 23 Cruz Vermelha Square, 7th Floor, Rio de Janeiro, RJ 20230-130, Brazil*

ABSTRACT

Radiotherapy remains a major approach to adjuvant therapy for patients with advanced colorectal cancer, however, the fractionation schedules frequently allow for the repopulation of surviving tumors cells, neoplastic progression, and subsequent metastasis. The aim of the present study was to analyze the transgenerational effects induced by radiation and evaluate whether it could increase the malignant features on the progeny derived from irradiated parental colorectal cancer cells, Caco-2, HT-29, and HCT-116. The progeny of these cells displayed a differential radioresistance as seen by clonogenic and caspase activation assay and had a direct correlation with survivin expression as observed by immunoblotting. Immunofluorescence showed that the most radioresistant progenies had an aberrant morphology, disturbance of the cell–cell adhesion contacts, disorganization of the actin cytoskeleton, and vimentin filaments. Only the progeny derived from intermediary radioresistant cells, HT-29, reduced the E-cadherin expression and overexpressed β-catenin and vimentin with increased cell migration, invasion, and metalloprotease activation as seen by immunoblotting, wound healing, invasion, and metalloprotease activity assay. We also observed that this most aggressive progeny increased the Wnt/β-catenin-dependent TCF/LEF activity and underwent an upregulation of mesenchymal markers and downregulation of E-cadherin, as determined by qRT-PCR. Our results showed that the intermediate radioresistant cells can generate more aggressive cellular progeny with the EMT-*like* phenotype. The Wnt/β-catenin pathway may constitute an important target for new adjuvant treatment schedules with radiotherapy, with the goal of reducing the migratory and invasive potential of the remaining cells after treatment. J. Cell. Biochem. 115: 2175–2187, 2014.

KEY WORDS: RADIORESISTANCE; COLORECTAL CANCER; EMT; Wnt/β-CATENIN PATHWAY

Colorectal cancer (CRC) is the second most commonly diagnosed cancer in women and the third in men being the fourth most common cause of cancer mortality worldwide [Jemal et al., 2011]. The 5-year survival rate for CRC is 90% if detected at localized stage, but this survival rate drops to 69.2% in intermediary stage and 11.7% for patients with metastatic disease [Siegel et al., 2012]. In Brazil, the statistics are in accord with the global incidence, as observed in recent data from the Brazilian National Institute of

Grant sponsor: CNPq; Grant number: 573806/2008-0; Grant sponsor: FAPERJ; Grant number: E-26/110.324/2012; Grant sponsor: Ministerio da Saude-Brazil.

*Correspondence to: José Andrés Morgado-Díaz, Cellular Biology Program, Brazilian National Cancer Institute (INCA), 37André Cavalcanti Street, 5th Floor, Rio de Janeiro, RJ 20230-051, Brazil. E-mail: jmorgado@inca.gov.br

Manuscript Received: 7 February 2014; Manuscript Accepted: 1 August 2014

Accepted manuscript online in Wiley Online Library (wileyonlinelibrary.com): 7 August 2014

DOI 10.1002/jcb.24896 • © 2014 Wiley Periodicals, Inc.

Cancer [Ministério da Saúde, 2011]. The molecular mechanisms of CRC development have been extensively studied, and multiple genetic and epigenetic aberrations are correlated with its progression. However, this is not sufficient for the development of good treatments at advanced stages of CRC. Radiotherapy (RT) is standard in clinical practice guidelines for the neo-adjuvant treatment of resected advanced rectal cancers. Protocols of RT consist of daily exposure to a hyperfractionated dose of approximately 1.8–2.0 Gy for 5–7 weeks or a hypofractionated dose of 5 Gy daily for 5 days, resulting in a total dose of 25 Gy [Pach et al., 2012]. Both fractionation schedules are important to allow for the recovery of normal tissues between RT-exposures. However, the repopulation of surviving tumor cells can occur, and the cure rate of CRC has remained low as a consequence of tumor recurrence, neoplastic progression, and metastasis, which frequently occur after radiotherapy [Camphausen et al., 2001; Kim and Tannock, 2005]

It is important to note that 90% of cancer mortality is attributed to metastasis and not due to the primary tumors from which these malignant lesions arose. Increased migratory and invasive potential, which allows malignant cells to spread from the primary tumor to distant organs, are two important hallmarks of cancer [Hanahan and Weinberg, 2011]. The epithelial cancer progression involves the early down regulation of epithelial markers and the acquisition of mesenchymal characteristics, such as changes in the organization of the actin cytoskeleton and acquisition of a fibroblast-*like* shape as well as increased cell migration and invasiveness properties [Thiery et al., 2009]. All these events characterize the epithelial-mesenchymal transition (EMT), a physiological process during embryonic development, wound-healing, and tissue repair and occurs in a pathological manner during epithelial tumor progression. Recent studies have been reported that the EMT is induced by growth factors and cytokines involved in tumor progression, such as EGF, TNF-α, and TGF-β [Andarawewa et al., 2011; Li et al., 2012] and the secretion of these growth factors and cytokines also have been reported after radiation exposure [Dent et al., 2003; Barcellos-Hoff et al., 2005]. Studies using cellular models, such as lung epithelial human A549 cells and HEC1A endometrial carcinoma cells have shown an EMT development in cells directly targeted by ionizing radiation [Jung et al., 2007; Tsukamoto et al., 2007]. However, it is known that following radiation exposure, cells do not die immediately, and the surviving cells continue interacting with their microenvironment and the post-irradiation behavior and phenotype of radioresistant cancer cells remain largely unknown. In addition, most of the studies analyzed the cells that were directly irradiated, and few recent studies have focused on the long-term and transgenerational effects induced by radiation [Harada et al., 2012]. In an in vivo context, molecular signatures of EMT have been found in the invasive front of advanced tumors [Peinado et al., 2007] and were correlated with chemo- and radio-therapeutic tumor resistance [Sabbah et al., 2008], that could be mediated by several mechanisms, including efflux pump upregulation, enhanced DNA repair, loss of p53 function, and alterations in the apoptotic pathway [Workman et al., 2013]. Moreover, resistance to therapy and invasion are considered distinct processes, but the signaling pathways underlying both invasion and resistance can overlap [Alexander and Friedl, 2012]; thus, studying the remaining cells after radiotherapy is relevant. Considering that (a) radioresistance and subsequent metastasis occur in nearly all patients who receive radiotherapy; (b) radiotherapy success is challenged by the survival and invasive capabilities of the remaining tumor cells that are not eradicated in the therapeutic window of the dose fractionation; and (c) radiotherapy remains a major therapeutic modality in cancer treatment, efforts to understand the molecular mechanisms that regulate these events are essential to the development of approaches to prevent or revert the therapeutic failure.

In the present study we analyzed the transgenerational effects induced by radiation in the progeny derived from irradiated parental colorectal cancer cells and evaluated whether the radiation could increase the malignant features such as migratory and invasiveness capabilities and the signaling pathways that are activated in the remaining cells after treatment.

MATERIALS AND METHODS

MATERIALS

The mouse anti-α-tubulin monoclonal antibody (Cat. no. 32–2500) was purchased from Invitrogen Inc. (Carlsbad, CA). The mouse anti-E-cadherin monoclonal antibody (36 clone, Cat. no. 610182) was purchased from BD Biosciences (San Diego, CA). The rabbit β-catenin, rabbit p-GSK3β (Ser-9) (5B3, Cat. no.9323), rabbit anti-GSK3β monoclonal (27C10, Cat. no. 9315), and rabbit anti-GAPDH antibodies (14C10, Cat. no. 2118) were purchased from Cell Signaling (Danvers, MA). The rabbit anti-survivin antibody (Cat. no. AF886) was purchased from R&D System (Minneapolis, MN). The Alexa Fluor® 488 goat anti-mouse IgG (Cat. no.A11001) and Alexa Fluor® 546 goat anti-rabbit IgG (Cat. No.A11010) were obtained from Molecular Probes (Eugene, Oregon). The horseradish peroxidase-conjugated anti-mouse (Cat. no. NA931) and anti-rabbit IgG (Cat. no.NA934), were purchased from GE Healthcare (Chalfont St. Giles, UK). The mouse anti-vimentin monoclonal antibody (clone V9, Cat. no. V6630), phalloidin–tetramethylrhodamine B isothiocyanate (Cat. no.P1951), mouse monoclonal anti-vimentin–Cy3 antibody (Cat. no. C9080) and 4′,6-diamidino-2-phenylindole dihydrochloride (DAPI; Cat. no. 32670) were purchased from Sigma–Aldrich (Saint Louis, MO).

CELL CULTURE AND TREATMENT WITH IONIZING RADIATION

The human colorectal adenocarcinoma cell lines Caco-2 (HTB-37™) and HT-29 (HTB-38™) and the human colorectal carcinoma cell line HCT-116 (CCL-247™) were obtained from the American Type Culture Collection (ATCC; Manassas, VA) and have been established in culture for many years. The Caco-2 cells harbor mutations in *APC*, *TP53*, and *SMAD4* and have a differentiated phenotype when they form a confluent monolayer, with low invasive and metastatic potential, while the HT-29 cells are moderately differentiated, with *BRAF*, *PIK3CA*, *TP53*, *SMAD4*, and *APC* mutations [Rowan et al., 2000; Flatmark et al., 2004]. The HCT-116 cells harbor *KRAS*, *PIK3CA*, and β-catenin mutated and are *TP53* wild type, with an undifferentiated phenotype and high tumorigenic potential [Ahmed et al., 2013]. The cells were maintained in DMEM (GIBCO-Invitrogen, Carlsbad, CA) supplemented with 10% heat-inactivated fetal bovine serum (FBS), penicillin G (60 mg/L), and streptomycin (100 mg/L) at

37 °C in a humidified atmosphere of 5% CO_2/95% air until they reached sub-confluency and were exposed to a single dose of radiation (5 Gy) at 25 °C using a 137Cs gamma irradiator (IBL 437C, CIS Bio International) at a dose rate of 2.65 Gy/min. The cells were confined in irradiated cell medium (irradiated group) or in non-irradiated cell medium (control group) for 24 h, and after this time, the cells were passaged with 0.05% trypsin/0.02% EDTA in PBS solution. The control and radiation surviving single cells were plated and maintained in DMEM with 10% FBS medium until progeny colonies formed and were then subjected to the subsequent experiments. The progeny derived from the unirradiated cells were called the "F1 Control," and the progeny derived from the irradiated cells were called the "F1 5Gy." Thus, all the experiments were performed with the first generation after radiation. For experimental purposes, the cells were seeded into culture flaks, plates, or glass coverslips or onto Polycarbonate Membrane Transwell® Inserts with an 8 μm pore size (Cat. no. 3422; Costar, Cambridge, MA) coated with Matrigel® (Cat. no. 356230; BD Biosciences, San Diego, CA). The DMEM medium in which the progeny derived from irradiated or control HT-29 cells were grown was called conditioned medium.

CLONOGENIC ASSAY

Progeny derived from irradiated and control parental cells (Caco-2, HT-29, and HCT-116), were seeded at a low density (2.5×10^2 cells) in 12-well plates for seven days to determine the effects of irradiation on their clonogenic potential. At this time, the colonies were fixed with ethanol for 10 min, stained with a crystal violet solution (0.05% crystal violet and 20% ethanol) for 10 min, washed twice with water and then solubilized with methanol. The absorbance at 595 nm was measured with a Spectra Max 190 spectrophotometer (Molecular Devices, Sunnyvale, CA), and the bar charts were plotted as the percentage of colony formation based on the optical density. Clonogenic assay in F1 5Gy HT-29 cells silenced to survivin was also performed.

CASPASE ACTIVITY

Progeny of irradiated and control parental cells (Caco-2, HT-29, and HCT-116) were seeded in a 96-well plate (5×10^3 cells/well) for 24 h. Then, 100 μL of Caspase-Glo® reagent (CaspaseGlo® 3/7 assay, Cat. no. G8091, Promega, Madison, WI) was added per well. The cells were incubated at room temperature for 1.5 h and 90 μL of the solutions (cell sample + CaspaseGlo® reagent) from each well were transferred to an opaque-walled 96-well plate. The luminescence was recorded with a luminometer Veritas (Turner Biosystems, Inc. Sunnyvale, CA). The data were plotted as the caspase 3,7 activation index (F1 5Gy/F1 Control).

SURVIVIN siRNA

HT-29 cells were transfected with either a non-targeting control siRNA scramble (siRNA negative control, Ambion, TX) as a control for non-sequence-specific effects, or survivin-specific siRNA sequence (Silencer Predesigned siRNA BIRC5, Qiagen), to a final siRNA concentration of 12 nM. The cells were transfected with Lipofectamine™ RNAi MAX (Invitrogen) according to the manufacturer's instruction and the survivin expression was verified by immunoblotting cell lysates.

CELL EXTRACTION AND IMMUNOBLOTTING

For Western blot analysis, the progeny derived from irradiated and control cells were homogenized in lysis buffer (1% Triton X-100, 0.5% sodium deoxycholate, 0.2% SDS, 150 mM NaCl, 2 mM EDTA, 10 mM Hepes, pH 7.4) containing 20 mM NaF, 1 mM orthovanadate, and a protease inhibitor cocktail (Cat.no.P8340, Sigma, MO, 1:100 dilution) for 30 min at 4 °C. The homogenized lysates were submitted to centrifugation at 10,000 g for 10 min at 4 °C. The supernatants were collected and stored at −80 °C for the subsequent analysis. Equal amounts of protein (30 μg/lane) from the total cell lysates were prepared by boiling after the addition of the denaturing sample buffer and were then electrophoretically separated by SDS-PAGE on 10% or 13% gels and transferred to nitrocellulose sheets. The membranes were blocked with 5% non-fat milk for 1 h and incubated overnight with primary antibodies against E-cadherin (1:5000), β-catenin (1:4000), vimentin (1:1000), phospho-GSK (1:1000), total GSK (1:1000), and survivin (1:1000). After washing, the membranes were incubated for 1 h with the appropriate secondary antibody for 1 h at room temperature. The membranes were washed, and the protein bands were visualized using an enhanced chemiluminescence kit (GE Healthcare UK Limited, Buckinghamshire, UK). The band images were quantified by optical density using LabWorks 4.6 software (Bio-Rad Laboratories, Hercules, CA). When indicated, the membranes were washed and reprobed with anti-α-tubulin (1:500) or anti-GAPDH (1:1000) antibodies as the protein loading control.

IMMUNOFLUORESCENCE AND ACTIN CYTOSKELETON DETECTION

F1 5Gy and F1 Control Caco-2 and HT-29 cells were grown in glass coverslips until they formed colonies. The cells were washed with PBS/CM (PBS containing 100 mM $CaCl_2$ and 100 mM MgCl2, pH 8.0) and fixed with methanol for 10 min at −20 °C. Then, the cells were rehydrated with PBS/CM, blocked with 0.2% BSA for 1 h, and permeabilized with 0.1% Triton X-100. The cells were incubated overnight at 4 °C with specific primary antibodies, anti-E-cadherin (1:300) and anti-β-catenin (1:200). Afterward, the cells were incubated with the appropriate Alexa Fluor® 488 anti-mouse or Alexa Fluor® 546 anti-rabbit secondary antibodies (1:500) for 1 h. Then, the cells were incubated with 4′,6-diamidino-2-phenylindole dihydrochloride (DAPI) (1:1000) for 3 min, washed and mounted using Propyl-Gallate (Sigma–Aldrich). To visualize the F-actin and vimentin subcellular distributions, the cell monolayers were fixed in 4% paraformaldehyde, permeabilized with 0.5% Triton X-100 and incubated in 500 ng/mL TRITC-phalloidin or anti-vimentin−Cy3 (1:300) for 40 min at room temperature followed by an incubation with 4′,6-diamidino-2-phenylindole dihydrochloride (DAPI) (1:1000) for 3 min. Then, the cell monolayers were washed and mounted using n-propyl-gallate. The glass coverslips were visualized in a confocal laser scanning microscope, FV10i-O and the images were analyzed using the FV10-ASW software (Olympus, Tokyo, Japan). The images are representative of three independent experiments.

WOUND HEALING ASSAY

F1 5Gy and F1 Control Caco-2 and HT-29 cells were seeded into a 24-well plate and allowed to grow until they reached confluency. Then, the cell monolayers were manually wounded by scraping with a

pipette tip to carry out the wound healing assay. For each well, five sites of a unique regular wound were analyzed under an Axio Observer.Z1 microscope (Carl Zeiss, Inc., Jena, Germany) equipped with an Axio Cam HRc and Axio Vision Release 8.2 Image Analyzer and then selected and marked. Then, the cells were permitted to migrate into the clearing area for 24 h. Immediately after wounding (t = 0 h) at the end of the experiment (t = 24 h), the entire wound of the five previous selected sites of each scrap/well were photographed, and the distance between the two edges of the injury were quantified using Adobe Photoshop Cs3 (Adobe Systems Inc., CA, EUA). The values of cell migration are represented as the percentages of cell migration in the bar graphs and the data are presented as the means ± SEM of triplicate assays for each cell line; at least three independent experiments were performed.

INVASION ASSAY

For the cell invasion assay, F1 5Gy and F1 Control Caco-2 and HT-29 cells (3×10^4) in 200 μL of serum-free medium were seeded in the upper surface of the Polycarbonate Membrane Transwell® Inserts with an 8 μm pore size (Costar), coated with 20 μL Matrigel® (BD Biosciences) diluted 1:10 in DMEM. DMEM with 10% FBS was added as a chemoattractant in the lower chamber, and after 24 h of incubation, the upper surface of the membrane was scrubbed with a cotton swab. The invaded cells in the lower membrane were fixed with ethanol for 10 min, stained with crystal violet and analyzed under the Axio Observer Z1 microscope. The number of invaded cells was expressed as the average of four random fields under the microscope. The values of cell invasion are represented as fold increases of cell invasion (where F1 Control = 1) in the bar graphs, and the data are presented as the means ± SEM of triplicate assays of three independent experiments.

ZYMOGRAPHY ASSAY

Equal protein amounts from the conditioned culture medium of the F1 Control and F1 5Gy HT-29 cells were subjected to SDS-PAGE in 10% (v/v) gels containing 0.2% gelatin (porcine skin, type A, Cat.No. G9136 Sigma–Aldrich Co). After electrophoresis, the gels were washed twice (30 min each time at room temperature) in 10 mM Tris/HCl, pH 8.8 containing 2.5% Triton X-100 and then incubated in activation buffer (5 mM $CaCl_2$, 0.02% NaN_3, and 50 mM Tris/HCl, pH 8.0) at 37 °C overnight. The next day, the gels were stained with Coomassie Brilliant Blue R-250 and destained in 10% (v/v) acetic acid and 40% (v/v) methanol. The gelatinolytic activity of the MMPs was detected as transparent bands on the blue background. The gels were scanned for quantification by optical density with the LabWorks 4.6 software (Bio-Rad).

TCF/LEF REPORTER TRANSCRIPTIONAL ASSAY

To analyze the transcriptional activity of β-catenin in the progeny, an analysis of the activation of the T-cell factor (TCF)/lymphoid enhancer factor (LEF) family of transcription factors (TCF/LEF) was performed using the Dual-Luciferase® Reporter Assay System Kit (Cat. no. E1910, Promega, Madison, WI). Two different TCF luciferase reporter genes were used in this assay: wild-type TCF-luciferase reporter construct (TOPflash) and a mutated TCF-luciferase reporter construct (FOPflash), which was used as a negative control for TOPflash activity. The progeny derived from control or irradiated Caco-2 and HT-29 cells were seeded (2×10^3) in a 24-well plate and grown until reaching sub-confluency. Then, the cells were co-transfected transiently with SUPER 8X TOP FLASH β-catenin Luciferase (2 μg) and PRL-TK (Renila 0.2 μg) plasmids or SUPER 8X FOP FLASH β-catenin Luciferase (2 μg) and PRL-TK (Renila 0.2 μg) plasmids. Both co-transfections were performed using the FuGENE® HD Transfection Reagent (Cat. no. E2311; Promega, WI), according to the manufacturer's protocol. Renilla luciferase and firefly luciferase activities were measured 24 h after transfection using the Dual Glo assay reagents (Promega), according to the manufacturer's protocol, in a luminometer Veritas (Promega). The results were normalized (Top activity/Rel activity)/(Fop activity/Rel activity), and the TCF/LEF reporter activities were plotted in bar graphs as fold-changes over the control. The data are presented as the means ± SEM of triplicate assays in three independent experiments.

RNA EXTRACTION AND QUANTITATIVE REAL-TIME REVERSE TRANSCRIPTION POLYMERASE CHAIN REACTION (QRT-PCR)

Changes in E-cadherin, Snail, Slug, Twist, Vimentin, Fibronectin and N-cadherin mRNA levels were measured by RT-qPCR. Total mRNA derived from the progeny of irradiated and control HT-29 cells were obtained using the Trizol® reagent (Cat. no. 15596-026, Invitrogen), according to the manufacturer's protocol. The mRNA was stored at −80 °C. Two micrograms of total mRNA was subjected to genomic DNA digestion with amplification grade I DNAse (Cat. no. 18068-015, Invitrogen) to remove genomic DNA contamination. The RNA was reverse transcribed to complementary DNA (cDNA) with the Superscript II Reverse Transcriptase (Cat. no. 18064-014, Invitrogen) and Oligo-dT18 (Cat. no. 18418-012, Invitrogen) kits. The reactions were performed using the SYBR Green PCR Kit (Cat. no. 204072, Qiagen) in a Rotor Gene Q thermocycler (Qiagen) with a hot-start stage step of 10 min at 95 °C followed by 45 cycles of 20 s at 95 °C, 30 s at 60 °C, and 30 s at 72 °C. The following primers were used: α-Actin, forward 5′-TACAATGAGCTGCGTGTGG-3′ and reverse 5′-TAGCACAGCCTGGATAGCAA-3′; E-cadherin, forward 5′-TGGCGTCT GTAGGAAGGCA′-3′ and reverse 5′-GGCTCTTTGACCACCGCTCT-3′; Snail, forward 5′-TCGGAAGCCTAACTACAGCGA-3′ and reverse 5′-AGATGAGCATTGGCAGCGAG-3′; Slug, forward 5′ AAGCATTTCAACGCCTCCAAA-3′ and reverse 5′-GGATCTCTGGTTGTGGTATGACA-3′; Twist, forward 5′-GGCACCATCCTCACACCTCT-3′ and reverse 5′-TGGCTGATTGGCACGACCT-3′; Vimentin, forward 5′-GCCAGATGCGTGAAATGGAA-3′ and reverse 5′-CTGTCCATCTCTAGTTTCAACCG-3; Fibronectin, forward 5′-CACCTTGAATGACAATGCTCGGAG-3′ and reverse 5′-GACCCAGGCTTCTCATACTTGATG-3′; N-cadherin, forward 5′- ACCAGGACTATGACTTGAGCC-3′ and reverse 5′-GGCGTGGATGGGTCTTT- CA-3′. The expression data were normalized to the housekeeping gene α-Actin and the data were plotted in a bar graph as the fold change of the mRNA expression of the F1 5Gy compared to the F1 Control. The data are presented as the means ± SEM of duplicate assays of three independent experiments.

STATISTICAL ANALYSIS

All quantitative data presented are the means ± SEM from at least three independent experiments. The statistical analysis and the

creation of the bar graphs were performed with Prism, 5.0 (GraphPad™ Software, San Diego, CA). The Student's t-test and the difference was considered statistically significant when $^{*}P < 0.05$; $^{**}P < 0.01$; $^{***}P < 0.001$.

RESULTS

COLORECTAL CANCER CELLS SHOW DIFFERENTIAL RADIOSENSITIVITY LEVELS WHICH ARE DIRECTLY CORRELATED WITH CASPASE ACTIVATION, SURVIVIN UPREGULATION, AND ABNORMAL CELL MORPHOLOGY IN THEIR PROGENIES

To evaluate the response to radiation exposure, human colorectal cancer cell lines Caco-2, HT-29, and HCT-116 were irradiated at sub-confluency, confined in the irradiation medium for 24 h, trypsinized and plated to permit progeny colony formation from the surviving single cells. Initially, we assessed the radioresistance level in these cells lines by using a clonogenic assay and observed that, among the three cell lines used, Caco-2 was more radioresistant than HT-29 and HCT-116, in this order (Fig. 1A). This result was corroborated by the Caspase-Glo® assay, which showed a differential induction of caspase activity in these cells. The progeny of the irradiated Caco-2 cell line showed a minor induction of caspase, whereas the progeny of irradiated HT-29 cells showed an intermediate caspase induction and the progeny of irradiated HCT-116 cells showed a major index of caspase induction (Fig. 1B) compared to the respective control progeny. Because it has been reported that a member of the inhibitor of apoptosis proteins (IAP) family, survivin, leads to the suppression of apoptosis via the direct or indirect inhibition of caspase-related proteins [Sah et al., 2006], we analyzed whether the expression of survivin is correlated with the differential induction of caspase in our study model. We observed that the most resistant progeny, F1 5Gy Caco-2 and F1 5Gy HT-29, showed an increase of survivin expression, whereas the F1 5Gy HCT-116 progeny (more radiosensitive) displayed a reduction of survivin expression (Fig. 1C). Additionally, to analyze if the survivin

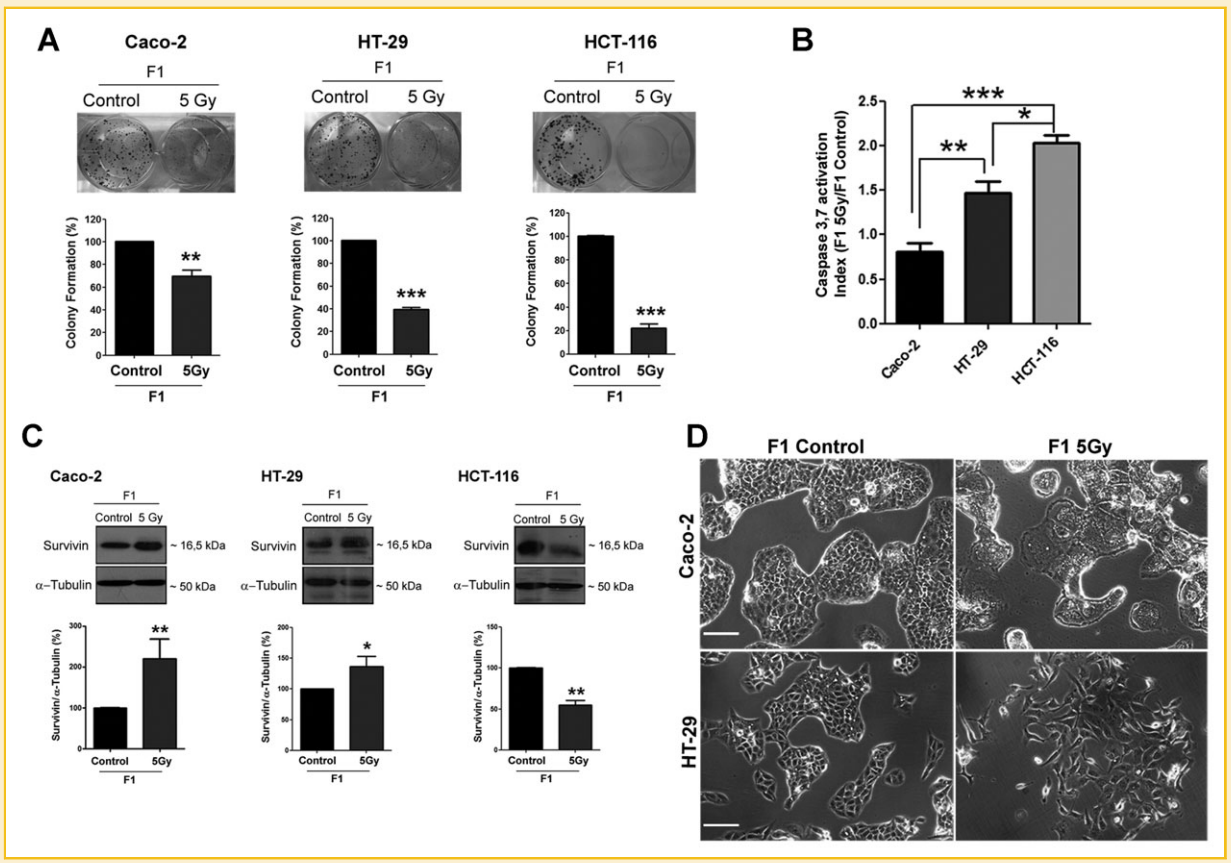

Fig. 1. Survival and Morphologic analysis of the progeny derived from parental irradiated cells. A: Representative images of the clonogenic assay of F1 Control and F1 5Gy of Caco-2, HT-29, and HCT-116 cells. Bar graphs are plotted as the percentages of colony formation after an optical density measurement (595 nm). B: Analysis of caspase 3 and 7 activation with the CaspaseGlo® assay. Bar graphs are representative of activation index (F1 5Gy/F1 Control) of Caco-2, HT-29, and HCT-116 cells. The data are presented as the means ± SEM of triplicate assays for each cell type of three independent experiments. C: Immunoblotting analysis of survivin expression in cell lysates of F1 Control and F1 5Gy of Caco-2, HT-29, and HCT-116 cells. Bar Graphs are normalized as the percentage of protein expression (where F1 Control = 100%), and α-tubulin protein was used as loading control. D: cell morphology of F1 Control and F1 5 Gy was analyzed by phase contrast microscopy. Images are representative of at least three experiments. Scale bar: 50 μm. The data are presented as the means ± SEM of triplicate assays for each cell type of three independent experiments. Significance was determined by a *t*-test. $^{*}P < 0.05$; $^{**}P < 0.01$; $^{***}P < 0.001$.

expression is involved in the maintenance of the progeny derived from irradiated cells, F1 5Gy HT-29 cells were knocked-down with si-RNA against survivin and analyzed the clonogenic potential. The results showed a drastic reduced colony formation in the F1 5Gy HT-29 silenced for survivin protein in relation to F1 5Gy HT-29 (Figs. S1A and S1B, supplementary results). Because the progeny of the Caco-2 and HT-29 were the cells most able to survive after irradiation, the subsequent experiments were performed with both cell lines to analyze the phenotypic behavior of their progeny after irradiation. Previous studies showed that radiation induced morphological changes in epithelial cells at early time points after treatment [de Carvalho et al., 2006; Andarawewa et al., 2007]. However, there are only a few studies that focused on the survival progeny at distant time points after radiotherapy. Therefore, we analyzed the cell morphology of the F1 5Gy Caco-2 and F1 5Gy HT-29 cells by optical microscopy. We observed that both progeny F1 5 Gy Caco-2 and F1 5Gy HT-29 displayed an abnormal colony formation compared with the F1 Control progeny (Fig. 1D). The F1 5Gy Caco-2 progeny showed abnormalities in morphology, such as an increase in cell volume and lamellipodia formation; however, the cohesive colony pattern was maintained 5 days after culturing. The F1 5Gy HT-29 progeny showed intense cell dispersion and the acquisition of a fibroblastic shape compared to the F1 Control HT-29 progeny. Together, these results suggested that Caco-2 and HT-29 cells are more radioresistant than HCT-116 cells and that this radioresistance could be correlated with lower caspase induction and survivin overexpression in the most radioresistant progeny, followed by acquisition of an aberrant phenotype.

IRRADIATION ALTERS THE SUBCELLULAR LOCALIZATION AND EXPRESSION OF THE EPITHELIAL MARKERS E-CADHERIN AND β-CATENIN IN THE PROGENY OF CELLS DERIVED FROM IRRADIATED SURVIVOR CELLS

The junction proteins are crucial for the maintenance of the epithelial architecture, and alterations in their expression and localization are involved in cancer progression. Thus, considering the abnormal morphology of the F1 5Gy Caco-2 and HT-29 cells (Fig. 1D), we analyzed the subcellular localization and the expression of the epithelial markers E-cadherin (Figs. 2A and B) and β-catenin (Figs. 2C and D) in these cells. Immunofluorescence images (Fig. 2A) obtained by confocal microscopy showed a well-defined labeling at the cell-cell contacts of E-cadherin in the F1 Control Caco-2 and HT-29 cells. However, the progeny derived from the irradiated survivor parental cells exhibited alterations at the subcellular localization of these adherent junctional proteins. The F1 5Gy Caco-2 cells displayed a discontinuous staining pattern of E-cadherin, but E-cadherin was still observed at the cell-cell contacts. The formation of a vesicular pattern in the cytoplasm indicated a possible E-cadherin internalization. The F1 5Gy HT-29 cells, which showed pronounced cell dissociation from each other, displayed an intense perinuclear localization of E-cadherin (Fig. 2A). The F1 Control Caco-2 and HT-29 cells showed a well-defined labeling of β-catenin at the cell-cell contacts; however, both progeny colonies of these irradiated cells showed an intense redistribution of this protein from the cell-cell contacts to the cytoplasm, including evident nuclear localization in the progeny of the irradiated HT-29 cells (Fig. 2C). Furthermore, we analyzed by immunoblotting the expression of E-cadherin and β-catenin of both progeny of the irradiated cells. We observed that the expression of E-cadherin was reduced in both progeny and that this effect was more pronounced in the F1 5Gy HT-29 cells (Fig. 2D). Regarding β-catenin, the densitometric analysis revealed a slight reduction of this protein in the F1 5Gy Caco-2 cells and a significant increase of this protein in the F1 5Gy HT-29 cells compared to the F1 Control of both cell lines (Fig. 2D). Together, these results showed that the progeny of the irradiated Caco-2 and HT-29 cells underwent alterations in the subcellular localization and expression of the epithelial markers E-cadherin and β-catenin.

PROGENY DERIVED FROM IRRADIATED PARENTAL CELLS UNDERGOES OVEREXPRESSION AND SUBCELLULAR REDISTRIBUTION OF VIMENTIN AND ACTIN CYTOSKELETON

Because we observed protein alterations at the cell–cell contacts and reduced expression of the epithelial marker E-cadherin, which could be related to EMT, we decide to analyze the distribution and expression of vimentin, an intermediate filament that is also considered to be an EMT marker and is expressed in metastatic cells [Sabbah et al., 2008]. An increased vimentin level was only observed in the F1 5Gy HT-29 cells, whereas both the F1 Control and F1 5Gy Caco-2 cells did not express this protein (Fig. 3A). Additionally, by immunofluorescence analysis, we observed a total redistribution of these filaments to the cell protrusions that accompanied the morphological alteration induced by the irradiation of the F1 5Gy HT-29 cells (Fig. 3B). Moreover, it is well known that the actin cytoskeleton modulates the loss of cell-cell contacts and migratory phenotype acquisition in epithelial cells that are experiencing a malignant progression, inducing membrane protrusions that are essential to cell migration and invasion, such as lamellipodia, filopodia, and invadopodia [Yamaguchi and Condeelis, 2007]. As our previous results showed alterations after irradiation related to tumor progression, such as an alteration of the distribution and expression of adherens junctional proteins and vimentin, we further analyzed the distribution pattern of the actin cytoskeleton in the progeny derived from the irradiated parental cells. By using TRITC-conjugated phalloidin and confocal microscopy, we observed that the F1 5Gy Caco-2 and F1 5Gy HT-29 cells displayed intense actin cytoskeleton reorganization (Fig. 3C). Despite the maintenance of the epithelial organization in the F1 5Gy Caco-2 cells, it was possible to observe the formation of cell membrane protrusions, such as lamellipodia, with a defined actin-rich leading edge and membrane ruffles. Moreover, the F1 5Gy HT-29 cells, which adopted a mesenchymal elongated shape, showed evident cell dispersion, with individual cells having restricting lamellipodia formation at the leading edge and long tail retraction, which are characteristics of highly migratory cells [Petrie et al., 2009]. These results showed that only the cells that adopted a mesenchymal-*like* shape, the F1 5Gy HT-29 cells, had increased vimentin expression and a redistribution of vimentin filaments throughout the cell protrusions. Indeed, the results indicate that the progeny of both irradiated cell lines underwent differential actin cytoskeleton reorganization related to the migratory potential compared to the progeny from unirradiated cells.

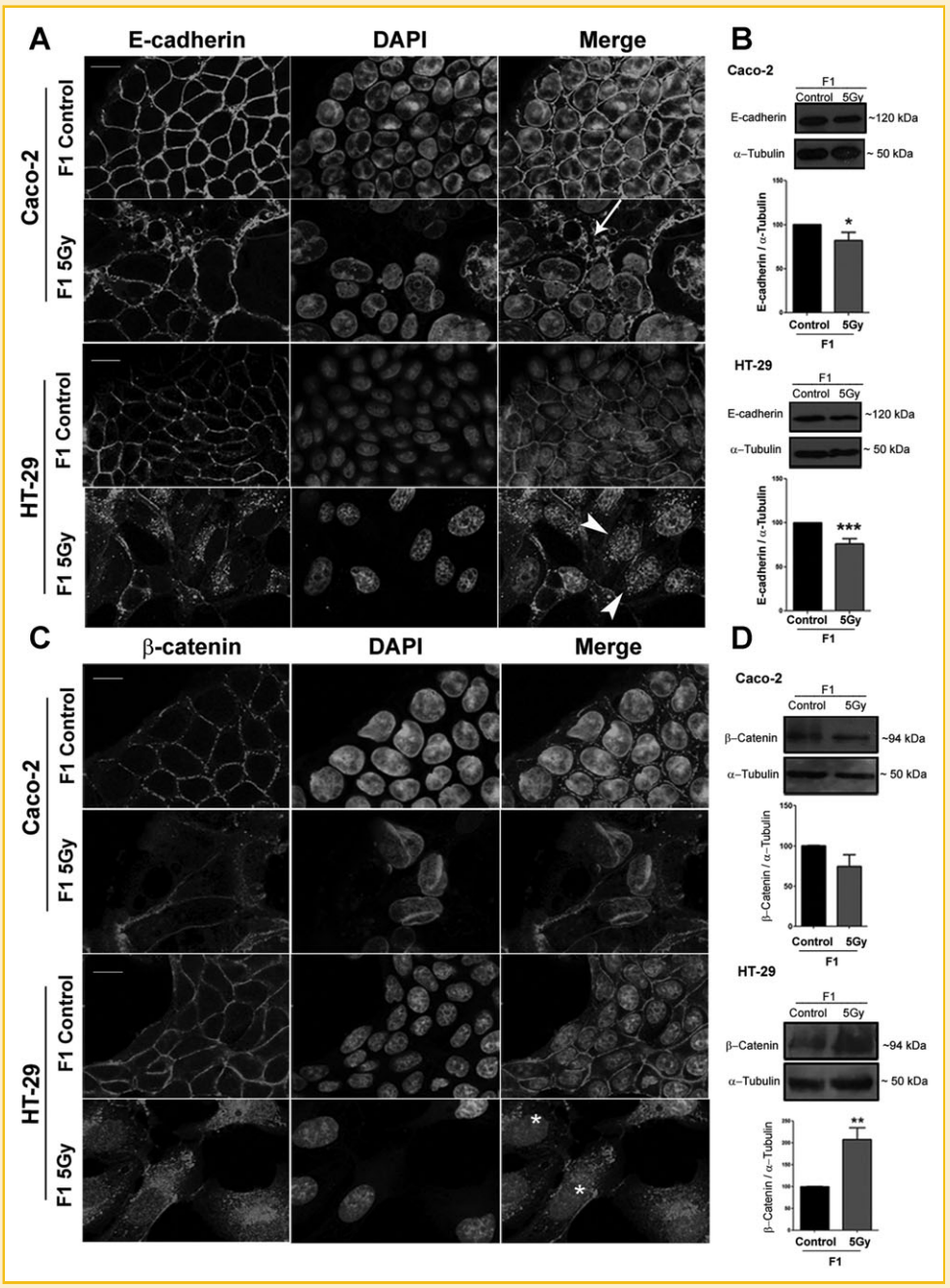

Fig. 2. Radiation effects on the subcellular localization and expression of E-cadherin and β-catenin in the progeny derived from irradiated cells. F1 Control and F1 5Gy of Caco-2 and HT-29 cells were grown in glass coverslips until colony formation and subjected to immunofluorescence analysis. Images are representative of at least three experiments. The nucleus was stained with DAPI. A: *Arrow*: E-cadherin internalized; *Arrowhead*: Clusters of cytosolic E-cadherin; Bar scale: 10 μm. C: *Asterisk*: nuclear β-catenin localization. Bar scale: 5 μm. Immunoblotting analysis of E-cadherin (B) and β-catenin (D) protein levels in lysates derived from F1 Control and F1 5Gy of Caco-2 and HT-29. Bar graphs are plotted as the percentage of protein expression (where F1 Control = 100%), and α-tubulin protein was used as loading control. The data are presented as the means ± SEM of triplicate assays for each cell type of three independent experiments. Significance was determined by t-test. $^{*}P < 0.05$; $^{**}P < 0.01$; $^{***}P < 0.001$.

PROGENY DERIVED FROM IRRADIATED HT-29 BUT NOT CACO-2 CELLS PRESENT INCREASED MIGRATORY AND INVASIVE POTENTIAL AS WELL AS INCREASED METALLOPROTEASE ACTIVITY

It is well documented that increased cell migration and invasiveness are characteristics of malignancy. Cell migration is driven by protrusive and contractile actin filaments structures, and the assembly of the cytoskeleton provides the force for plasma membrane protrusions [Tojkander et al., 2011]. In this context, to evaluate whether the radiation-induced cytoskeleton reorganization observed in the progeny of Caco-2 and HT-29 cells is related to increased cell migration, we performed a wound healing assay. We observed a reduction of the migratory potential in the F1 5Gy Caco-2 cells, whereas the F1 5Gy HT-29 cells presented an increase in cell migration (Figs. 4A and B, respectively). Next, we assessed the

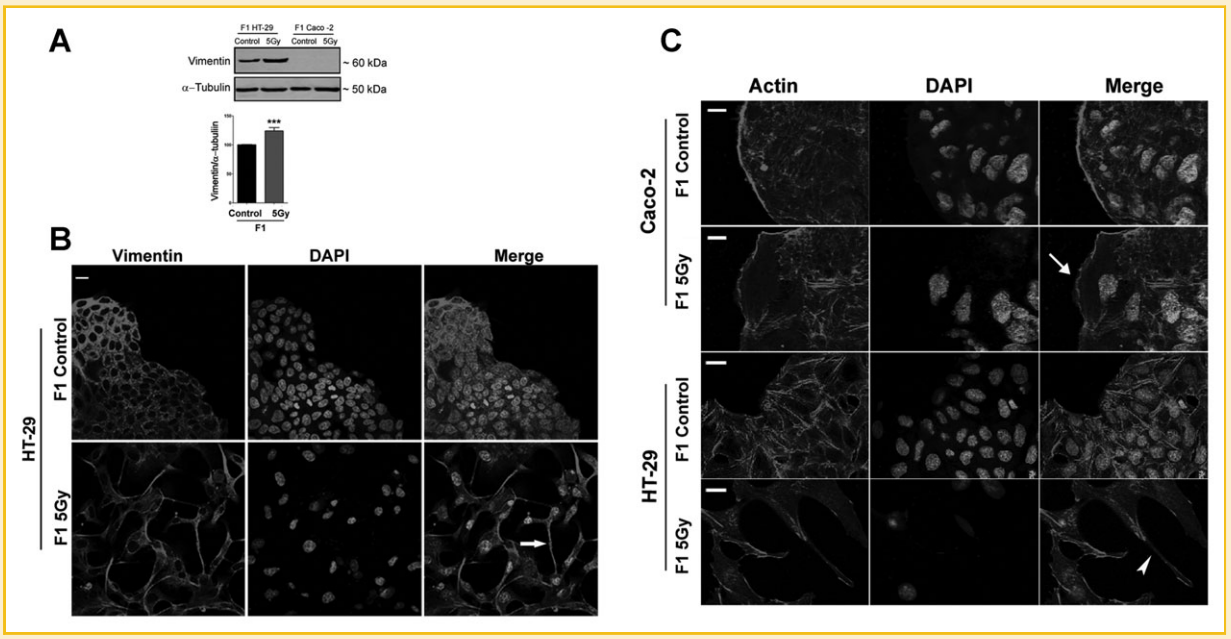

Fig. 3. Vimentin expression and subcellular localization and distribution of Actin cytoskeleton in the progeny derived from irradiated cells. A: Immunoblotting analysis of vimentin protein levels in F1 Control and F1 5Gy of Caco-2 and HT-29 cell lysates. Bar graphs are plotted as the percentage of protein expression (where F1 Control = 100%), and α-tubulin protein was used as loading control. The data are presented as the means ± SEM of triplicate assays for each cell type of three independent experiments. Significance was determined by t-test. ***$P < 0.001$. B: F1 Control and F1 5Gy of HT-29 cells were grown on glass coverslips until colony formation and subjected to immunofluorescence analysis of vimentin localization. Nucleus stained with DAPI. Images are representative of at least three experiments. *Arrow*: vimentin localization at cell protrusion; Bar scale: 10 μm. C: F1 Control and F1 5Gy of Caco-2 and HT-29 cells were grown on glass coverslips until colony formation, fixed, and stained for F-actin. Confocal images show the actin cytoskeleton distribution and cell protrusion formation. Nucleus was stained with DAPI. Images are representative of at least three experiments. *Arrow:* lamellipodia. *Arrowhead:* tail retraction. Bar scale: 10 μm.

invasiveness capacity of these progeny and we observed that only the cells that developed a higher migratory potential, F1 5Gy HT-29, also displayed a high invasive potential compared to the F1 Control cells (Fig. 4C). Furthermore, we evaluated the metalloprotease activity in these progeny by zymography. Metalloprotease-2 activity was increased in the F1 5Gy HT-29 cells compared to the F1 Control HT-29 cells, whereas no significant changes were observed for metalloprotease-9 (Fig. 4D). Together, these results showed that only the survival progeny of irradiated HT-29 cells developed an increase in cell migration, high invasive potential and increased metalloprotease activity.

PROGENY DERIVED FROM IRRADIATED HT-29 CELLS SHOWS AN INCREASE OF GSK-3β PHOSPHORYLATION AND *TCF-LEF* ACTIVITY FOLLOWED BY UPREGULATION OF MESENCHYMAL MARKERS AND E-CADHERIN DOWNREGULATION

Our previous results showed both an increased expression and nuclear labeling of β-catenin in the F1 5Gy HT-29 cells (Figs. 2C and D). The nuclear localization of β-catenin is related to activation of the Wnt/beta-catenin pathway, and a member of that pathway, glycogen synthase-3β (GSK-3β), plays an important role in the maintenance of the β-catenin cytoplasmic pools. GSK-3β activity is regulated by phosphorylation, and its inhibition is the result of its phosphorylation at its 9th serine residue (Ser-9), which prevents β-catenin degradation and induces cytoplasmic accumulation and posterior nuclear translocation. In the nucleus, this protein binds to the TCF/LEF promoter region and dramatically increases the transcriptional activity of genes that regulate processes, such as survival, migration, and invasion [Luo, 2009]. Thus, to analyze the involvement of this pathway as a consequence of nuclear β-catenin accumulation observed in the F1 5Gy HT-29 cells, we initially evaluated the phosphorylation status of GSK-3β by immunoblotting using an antibody that recognizes the inactive form of GSK-3β (phosphorylated at Ser-9). Figure 5A showed no alteration in the SER-9 phosphorylation status in F1 5Gy Caco-2 but increased levels of p-GSK3-β in the F1 5Gy HT-29 cells compared to the F1 HT-29 Control cells. Next, to evaluate if decreased activity of GSK3-β is related to the nuclear transcriptional activity of β-catenin, we performed a luciferase assay to analyze the TCF/LEF promoter activity. We observed an increase in the TCF/LEF promoter activity of approximately sevenfold in the F1 5Gy HT-29 cells compared to the F1 Control HT-29 cells (Fig. 5B) and a reduction of this activity in F1 5Gy Caco-2 cells. Increasing in the migration and invasion abilities of tumor cells are correlated with the EMT process, during which epithelial markers are downregulated and mesenchymal markers are up-regulated. To further analyze if the most malignant progeny that increased the cell migration and invasion abilities (F1 5Gy HT-29 cells) could develop malignant features related to an EMT process, we analyzed the expression of genes related to a mesenchymal phenotype (Snail, Slug, Twist, Vimentin, Fibronectin, and N-cadherin) and used the gene E-cadherin as an epithelial marker. Figure 5C shows a significant reduction of the E-cadherin

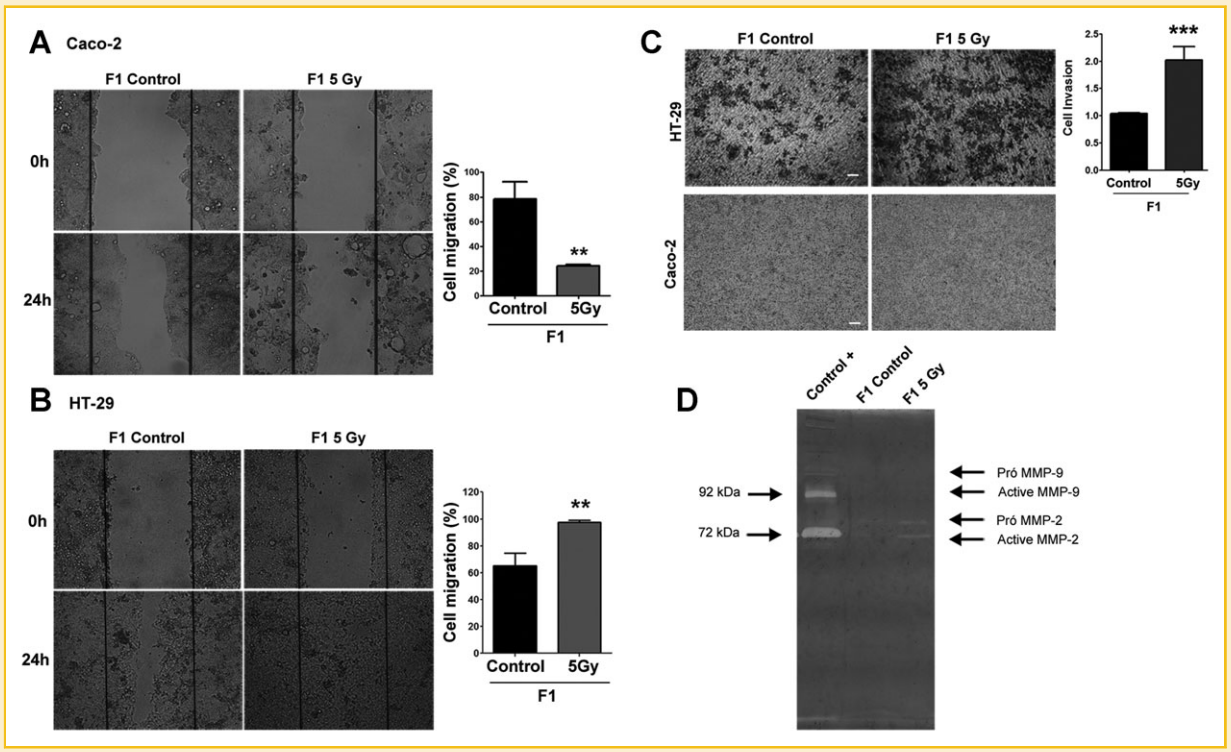

Fig. 4. Migratory and invasiveness analysis of the progeny derived from irradiated cells. F1 Control and F1 5Gy of Caco-2 (A) and F1 Control and F1 5Gy of HT-29 (B) cells were grown until confluence and subjected to wound healing assay. Bar graphs are plotted as percentages of cell migration. The data are presented as the means ± SEM of triplicate assays for each cell line of three independent experiments. Significance was determined by a *t*-test $^{**}P < 0.01$. C: F1 Control and F1 5Gy of Caco-2 and F1 Control and F1 5Gy of HT-29 cells were plated in Boyden chambers, coated with Matrigel® and subjected to invasion assay. Bar graphs are plotted as the fold increase of cell invasion (where F1 Control = 1). The data are presented as the means ± SEM of triplicate assays for each cell line of three independent experiments. Significance was determined by a *t*-test $^{***}P < 0.001$. D: Conditioned culture medium of the F1 Control and F1 5Gy of HT-29 cells were subjected to zymography assay. The image is representative of at least two experiments.

mRNA level and an increase of the Snail, Slug, and Fibronectin mRNA levels. The mRNA levels of Twist and N-cadherin were increased, but not in a significant manner, whereas the mRNA expression of Vimentin did not change. Together, these results showed that the most invasive progeny derived from parental irradiated HT-29 cells had an increase of β-catenin cytoplasmic pools and translocation of β-catenin to the nucleus (Figs. 2C and D), where it could activate the transcriptional activity of genes related to the WNT pathway and induced an EMT-related gene expression profile, mediated by GSK-3β activity.

DISCUSSION

The therapeutic strategies for CRC involve chemotherapy, radiotherapy, and surgery in patients with later stages of the disease. Although preoperative radiotherapy has been shown to reduce the local recurrence of CRC, the mortality rate is still high, 40–70% for stage II and III patients [Sebag-Montefiore et al., 2009]. Moreover, patients who develop a local recurrence after previous RT have significantly shorter survival expectancies and simultaneous distant metastasis than patients with local recurrence who have not received RT for their primary tumor [van den Brink et al., 2004]. The schedule of fractionated sub-lethal doses in clinical practices leads to a therapeutic window that can promote the microenvironment interactions of these cells, promoting repopulation and cell migration of the radiation-surviving cancer cells [Wong et al., 2010]. The molecular mechanisms by which this occurs remain to be defined. Although in vitro studies have shown the radiation-effects in early periods after treatment [de Carvalho et al., 2006; Andarawewa et al., 2007], only a few studies were focused on the reminiscent cells that escape from radiation-induced cell death.

In the present study, we analyzed the progeny derived from colorectal cancer cell radiation survivors according to the phenotypes and genotypes of the features related to malignant progression. Initially, we analyzed the radiosensitivity of colorectal cancer cells and observed that the most differentiated cell line, Caco-2, and the moderately differentiated cell line, HT-29, were more radioresistant than the undifferentiated cell line, HCT-116. It is estimated that *TP53* is mutated in 40–50% of CRCs [López et al., 2012]; therefore, it is important to analyze the treatment response in cells with different patterns of p53 expression. *TP53* is wild type in HCT-116 cells and is mutated in Caco-2 cells, that impairs caspase induction in these cells [Andarawewa et al., 2007]. *TP53* is also mutated in HT-29 cells; however, this mutation induces

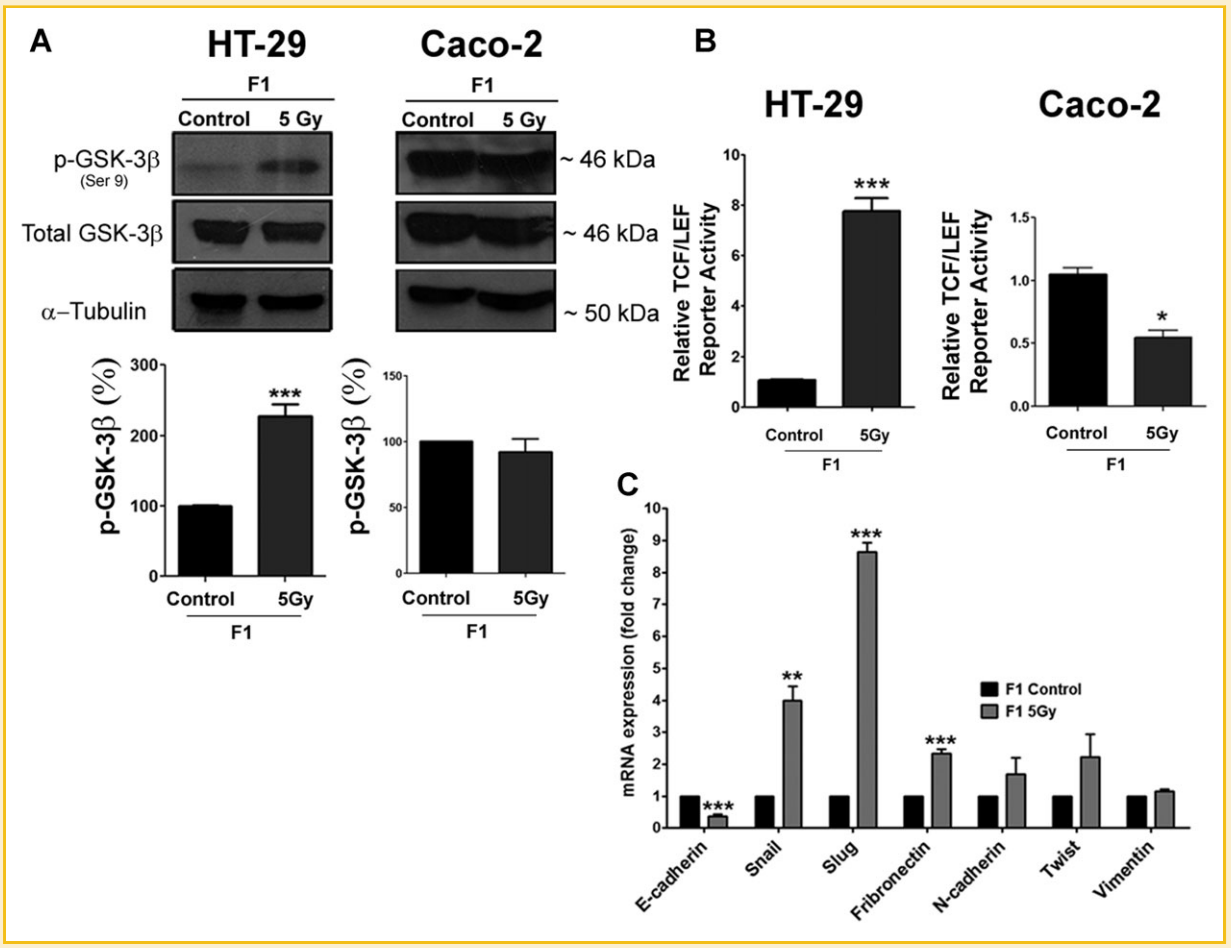

Fig. 5. GSK-3β phosphorylation status, TCF-LEF activity, and gene expression related to mesenchymal features in the progeny derived from irradiated cells. A: Immunoblotting analysis of GSK-3β phosphorylation and total protein level in F1 Control and F1 5Gy Caco-2 and HT-29 cells. Bar graphs are plotted as the percentage of protein expression (where F1 Control = 100%), and α-tubulin protein was used as a loading control. The data are presented as the means ± SEM of triplicate assays of three independent experiments. Significance was determined by a t-test. ***$P < 0.001$. B: F1 Control and F1 5Gy of Caco-2 and HT-29 cells were subjected to a Luciferase Reporter Assay to measure *TCF/LEF* activity. Bar graphs are plotted as the fold increase in F1 5Gy cells of reporter activity compared to F1 Control cells. C: RT-qPCR analysis of gene expression of genes related to a mesenchymal phenotype (Snail, Slug, Twist, Vimentin, Fibronectin, and N-cadherin) and the E-cadherin gene, an epithelial marker. Bar graphs are plotted as the fold change of F1 5Gy HT-29 cell mRNA expression compared to F1 Control HT-29 cell mRNA expression.The data are presented as the means ± SEM of triplicate assays of three independent experiments. Significance was determined by a t-test. **$P < 0.01$; ***$P < 0.001$.

an overproduction of a non-functional TP53 protein with an increased half-life [Aurelio et al., 2000], resulting in an intermediate caspase induction. Thus, the *TP53* status in these cells could explain the differential caspase induction after irradiation observed in the present study. Survivin is an inhibitor of apoptosis (IAP) family protein, which is a key regulator of apoptosis and is up regulated in most human tumors but undetectable in differentiated cells. In addition, this protein is related to therapeutic resistance, playing an important role in the drug and radiation resistant phenotype of human cancer cells [Mita et al., 2008]. Because the radiosensitivity levels were different in these cell lines, we analyzed survivin protein expression and interestingly, we observed increased survivin expression in the most radioresistant progeny, F1 5Gy Caco-2 and F1 5Gy HT-29, and a drastic reduction of survivin expression in the most radiosensitivity progeny, F1 5Gy HCT-116. High survivin expression in tumors is related to treatment failure in clinical studies [Stauber et al., 2007], poor prognosis and pro-metastatic phenotype in CRC patients [Krieg et al., 2013]. Additionally, the overexpression of survivin is involved in the disruption of apoptosis, and this impairment of apoptotic cell death may negatively affect the response of tumor cells to therapy. To evaluate the role of survivin in the maintenance of the progeny derived from irradiated cells, F1 5Gy HT-29 cells were silenced for the survivin protein using a siRNA and subjected to clonogenic assay. The results showed a reduction in the clonogenic capability of the F1 5 Gy + siRNA survivin in relation to F1 5Gy HT-29 progenies (Figs. S1A and S1B). Thus, the present results on survivin protein expression indicate its important role in the maintenance of survival cells after radiotherapy.

In addition to cell death resistance, disruption of the cell–cell adhesion system and the altered expression of E-cadherin and β-catenin, are related to cancer progression and metastasis. Our results showed intense abnormalities in the colony morphology of the most

radioresistant cells, F1 5Gy Caco-2 and F1 5Gy HT-29, (Fig. 1D) which were closely related to the subcellular mislocalization and altered expression of the epithelial markers E-cadherin and β-catenin (Fig. 2). We observed a slight discontinuous staining of E-cadherin with few membrane vesicles, suggesting protein endocytosis in the F1 5Gy Caco-2 cells [Palacios et al., 2005]. Additionally, we did not observe a significant alteration of the β-catenin expression in the F1 5Gy Caco-2 cells, only a diffuse cytosolic staining of this protein, with the colony cohesive pattern still maintained in this progeny. A prominent cell–cell adhesion disturbance was observed in the F1 5Gy HT-29 cells, where the cytoplasmic staining and cluster formations of E-cadherin were obvious. The downregulation of E-cadherin observed in the current study by immunoblotting is in agreement with the results of previous studies that described these E-cadherin protein clusters as the center of proteosomal degradation [Kopito, 2000]; Indeed, we observed an increased expression and nuclear localization of β-catenin in the F1 5Gy HT-29 cells. Increased β-catenin expression and its nuclear accumulation at the invasive front of colorectal cancers and in the scattered cells in the stroma suggest an EMT in these cells, with the progressive loss of E-cadherin and the acquisition of mesenchymal markers, as has been previously reported [Fodde and Brabletz, 2007]. Previous in vitro studies showed disturbances in the cell–cell adhesion of colorectal cancer cells induced by radiation soon after treatment [de Carvalho et al., 2006]. Here, we report, for the first time, the effects of radiation on cell–cell adhesion in the colorectal cancer cells remaining after radiation treatment. To further analyze the malignant phenotype of the progeny derived from irradiated cells we analyzed the vimentin protein, a mesenchymal marker that is expressed in metastatic cells [Wei et al., 2008]. We observed that only the progeny with intense cell dispersion, the F1 5Gy HT-29 cells, showed increased vimentin expression and subcellular redistribution accompanying the cell protrusions. In agreement with this observation, previous studies reveled that vimentin enhances cell migration and stabilized myosin during cell protrusion formation [Lund et al., 2010]. We also observed an intense formation of cell protrusions, such as lamellipodia with defined ruffles at the leading edge, in the F1 5Gy Caco-2 cells, although the adhesive properties of these colonies were maintained. Moreover, the F1 5Gy HT-29 progeny had individual cells with restricted lamellipodia formation at the leading edge as well as a long tail retraction with a mesenchymal elongated shape and evident cell dispersion, all of which are characteristics of highly migratory cells [Petrie et al., 2009].

As cell–cell junction disturbances and cytoskeleton reorganization with membrane projection structures could increase migration capabilities, we performed a cell migration assay. The F1 5Gy Caco-2 cells showed a slow cellular migration, and this could be related to the large leading edge of the lamellipodia, which produce multivector forces resulting in random cell migration [Petrie et al., 2009; Friedl et al., 2012]. On the other hand, the intermediate radioresistant progeny, the F1 5Gy HT-29 cells, showed increased cell migration in accordance with the observed cell protrusions and the fibroblastic-*like* shape of the cells, which induces a dominant and directionally leading edge protrusion, enhancing directed migration [Petrie et al., 2009]. It is known that vimentin increases the ability to generate the driving force of the actin filaments through the phosphorylation of the VASP protein, an inhibitory protein of actin capping, enabling the actin elongation that is necessary for membrane protrusion formation [Lund et al., 2010]. Therefore, we suggest that the increased expression and subcellular localization of vimentin in the F1 5Gy HT-29 cells acts with the increased migratory potential of this progeny. It is well known that a fibroblast-*like* cell morphology is thought to promote cell migration and the invasion of metastatic cells when they are undergoing EMT. Regarding clinical features, single cells or small clusters of de-differentiated tumor cells at the invasive front of colorectal cancers are represented by tumor budding, and this has been proposed to be a histological hallmark of EMT, particularly in the setting of colorectal carcinoma [Mitrovic et al., 2012].

In addition to an increase in cell migration, we observed that the F1 5Gy HT-29 cells also increased in invasiveness and matrix metalloproteinase-2 (MMP) activity. MMPs have critical roles in cell migration and invasion, and their upregulation is associated with tumor progression, poor differentiation, invasive stage, metastasis, and poor prognosis [Deryugina and Quigley, 2006]. Moreover, MMP-2 activity is increased in colorectal cancer and after fractionated 5 Gy preoperative radiotherapy in patients with colorectal cancer [Kumar et al., 2000; Herszényi et al., 2012]. Multiple transcriptional pathways are activated after E-cadherin loss, including those related to β-catenin activity [Sabbah et al., 2008]. For instance, there is evidence that at the invasive front of colorectal cancer, β-catenin accumulates in the cytoplasm and leads to its nuclear translocation, which activates the Wnt/beta-catenin pathway [Fodde and Brabletz, 2007]. Because nuclear β-catenin was observed in the F1 5Gy HT-29 cells, we analyzed the events related to Wnt/beta-catenin activation. We observed increased GSK-3β phosphorylation and TCF/LEF activity, indicating that there was transcriptional activity of β-catenin in the F1 5Gy HT-29 cells. Aberrant Wnt signaling have been found in human tumorigenesis and has been related to activate MMPs, becoming a promise target in pharmacological intervention [Wu et al., 2007; Verkaar and Zaman, 2011]. Indeed, the most studies linked the inhibition of this pathway only to reduce tumor growth, but not for reduction of invasiveness potentials.

Some studies have shown that this signaling pathway is related to EMT development, where many genes that regulate the epithelial features, such as polarity, cell adhesion, mesenchymal phenotype acquisition, cell migration, and invasion, are transcriptionally altered [Sabbah et al., 2008]. Thus, we evaluated whether the acquisition of cell migration and invasiveness by the F1 5Gy HT-29 cells was correlated with the development of an EMT phenotype by performing qRT-PCR to analyze the gene expression of the markers of these processes. We observed a reduction of mRNA E-cadherin with a concomitant increase of its repressors, Snail, Slug, and Twist. Indeed, we observed an increase in the mesenchymal markers Fibronectin and N-cadherin. Previous studies were performed related to EMT development after radiation in a xenograft model of hepatocellular carcinoma and showed the occurrence of later metastasis, suggesting the metastatic potential of residual tumor cells after treatment [Li et al., 2011]. Cancer cells may undergo adaptive changes following radiotherapy and that these adaptive changes may involve, at least in part, the EMT. Although most

studies describe any alteration related to the acquisition of a fibroblastic cell shape as being an EMT, here we considered the acquisition of an EMT-*like* phenotype in F1 5Gy HT-29 cells. The complete loss of epithelial markers and the gain of mesenchymal markers is rarely observed, and a partial EMT with dedifferentiation that is not fully complete, for example by the remaining expression of E-cadherin observed in this study, in the most migratory and invasive progeny, the F1 5Gy HT-29 cells (Fig. 3B).

In summary, we showed the transgenerational effects induced by radiation in the progeny derived from irradiated parental cells of colorectal cancer. Our results demonstrate that the intermediate radioresistant cells can generate cellular progeny that are more aggressive with EMT-*like* characteristics, and this explains, at least partially, the cancer progression related to the radioresistance of tumor cells. Therefore, not necessarily the most radioresistant phenotype acquires malignant advantages to migrate and invade after surviving the treatment. This is an important observation given the tumor heterogeneity, which coexist cells in various degrees of differentiation and malignant capabilities and the studies consider only the most resistant cells such as new target for increase the therapeutic successfully. Additionally, we suggest that the components of the Wnt/β-catenin cell signaling pathway could constitute important targets for new adjuvant treatment schedules with radiotherapy, with the goal of reducing the migratory and invasive potential of the remaining cells after radiotherapy.

ACKNOWLEDGMENT

We thank to the employers at the Hemoterapy Department of Brazilian National Cancer Institute for the use of the Gamma irradiator.

REFERENCES

Ahmed D, Eide PW, Eilertsen IA, Danielsen SA, Eknæs M, Hektoen M, Lind GE, Lothe RA. 2013. Epigenetic and genetic features of 24 colon cancer cell lines. Oncogenesis 2:e71.

Alexander S, Friedl P. 2012. Cancer invasion and resistance: interconnected processes of disease progression and therapy failure. Trends Mol Med 18:13–26.

Andarawewa KL, Costes SV, Fernandez-Garcia I, Chou WS, Ravani SA, Park H, Barcellos-Hoff MH. 2011. Lack of radiation dose or quality dependence of epithelial-to-mesenchymal transition (EMT) mediated by transforming growth factor β. Int J Radiat Oncol Biol Phys 79:1523–1531.

Andarawewa KL, Erickson AC, Chou WS, Costes SV, Gascard P, Mott JD, Bissell MJ, Barcellos-Hoff MH. 2007. Ionizing radiation predisposes nonmalignant human mammary epithelial cells to undergo transforming growth factor beta induced epithelial to mesenchymal transition. Cancer Res 67:8662–8670.

Aurelio ON, Kong XT, Gupta S, Stanbridge EJ. 2000. P53 mutants have selective dominant-negative effects on apoptosis but not growth arrest in human cancer cell lines. Mol Cell Biol 20:770–778.

Barcellos-Hoff MH, Park C, Wright EG. 2005. Radiation and the microenvironment - tumorigenesis and therapy. Nat Rev Cancer 5:867–875.

Camphausen K, Moses MA, Beecken WD, Khan MK, Folkman J, O'Reilly MS. 2001. Radiation therapy to a primary tumor accelerates metastatic growth in mice. Cancer Res 61:2207–2211.

de Carvalho AD, de Souza W, Morgado-Díaz JA. 2006. Morphological and molecular alterations at the junctional complex in irradiated human colon adenocarcinoma cells Caco-2. Int J Radiat Biol 82:658–668.

Dent P, Yacoub A, Contessa J, Caron R, Amorino G, Valerie K, Hagan MP, Grant S, Schmidt-Ullrich R. 2003. Stress and radiation-induced activation of multiple intracellular signaling pathways. Radiat Res 159:283–300.

Deryugina EI, Quigley JP. 2006. Matrix metalloproteinases and tumor metastasis. Cancer Metastasis Rev 25:9–34.

Flatmark K, Maelandsmo GM, Martinsen M, Rasmussen H, Fodstad Ø. 2004. Twelve colorectal cancer cell lines exhibit highly variable growth and metastatic capacities in an orthotopic model in nude mice. Eur J Cancer 40:1593–1598.

Fodde R, Brabletz T. 2007. Wnt/beta-catenin signaling in cancer stemness and malignant behavior. Curr Opin Cell Biol 19:150–158.

Friedl P, Locker J, Sahai E, Segall JE. 2012. Classifying collective cancer cell invasion. Nat Cell Biol 14:777–783.

Hanahan D, Weinberg RA. 2011. Hallmarks of cancer: the next generation. Cell 144:646–674.

Harada H, Inoue M, Itasaka S, Hirota K, Morinibu A, Shinomiya K, Zeng L, Ou G, Zhu Y, Yoshimura M, McKenna WG, Muschel RJ, Hiraoka M. 2012. Cancer cells that survive radiation therapy acquire HIF-1 activity and translocate towards tumour blood vessels. Nat Commun 3:783.

Herszényi L, Hritz I, Lakatos G, Varga MZ, Tulassay Z. 2012. The behavior of matrix metalloproteinases and their inhibitors in colorectal cancer. Int J Mol Sci 13:13240–13263.

Jemal A, Bray F, Center MM, Ferlay J, Ward E, Forman D. 2011. Global cancer statistics. CA Cancer J Clin 61:69–90.

Jung JW, Hwang SY, Hwang JS, Oh ES, Park S, Han IO. 2007. Ionising radiation induces changes associated with epithelial-mesenchymal transdifferentiation and increased cell motility of A549 lung epithelial cells. Eur J Cancer 43:1214–1224.

Kim JJ, Tannock IF. 2005. Repopulation of cancer cells during therapy: an important cause of treatment failure. Nat Rev Cancer 5:516–525.

Kopito RR. 2000. Aggresomes, inclusion bodies and protein aggregation. Trends Cell Biol 10:524–530.

Krieg A, Werner TA, Verde PE, Stoecklein NH, Knoefel WT. 2013. Prognostic and clinicopathological significance of survivin in colorectal cancer: a meta-analysis. PLoS ONE 8(6):e65338.

Kumar A, Collins HM, Scholefield JH, Watson SA. 2000. Increased type-IV collagenase (MMP-2 and MMP-9) activity following preoperative radiotherapy in rectal cancer. Br J Cancer 82:960–965.

Li CW, Xia W, Huo L, Lim SO, Wu Y, Hsu JL, Chao CH, Yamaguchi H, Yang NK, Ding Q, Wang Y, Lai YJ, LaBaff AM, Wu TJ, Lin BR, Yang MH, Hortobagyi GN, Hung MC. 2012. Epithelial-mesenchymal transition induced by TNF-α requires NF-κB-mediated transcriptional upregulation of Twist1. Cancer Res 72:1290–1300.

Li T, Zeng ZC, Wang L, Qiu SJ, Zhou JW, Zhi XT, Yu HH, Tang ZY. 2011. Radiation enhances long-term metastasis potential of residual hepatocellular carcinoma in nude mice through TMPRSS4-induced epithelial-mesenchymal transition. Cancer Gene Ther 18:617–626.

Lund N, Henrion D, Tiede P, Ziche M, Schunkert H, Ito WD. 2010. Vimentin expression influences flow dependent VASP phosphorylation and regulates cell migration and proliferation. Biochem Biophys Res Commun 395:401–406.

Luo J. 2009. Glycogen synthase kinase 3β (GSK3-β) in tumorigenesis and cancer chemotherapy. Cancer Lett 273:194–200.

López I, P Oliveira L, Tucci P, Alvarez-Valín F, A Coudry R, Marín M. 2012. Different mutation profiles associated to P53 accumulation in colorectal cancer. Gene 499:81–87.

Ministério da Saúde. 2011. Estimativa 2012: incidência de câncer no Brasil. Brazil: Rio de Janeiro.

Mita AC, Mita MM, Nawrocki ST, Giles FJ. 2008. Survivin: key regulator of mitosis and apoptosis and novel target for cancer therapeutics. Clin Cancer Res 14:5000–5005.

Mitrovic B, Schaeffer DF, Riddell RH, Kirsch R. 2012. Tumor budding in colorectal carcinoma: time to take notice. Mod Pathol 25:1315–1325.

Pach R, Kulig J, Richter P, Gach T, Szura M, Kowalska T. 2012. Randomized clinical trial on preoperative radiotherapy 25Gy in rectal cancer–treatment results at 5-year follow-up. Langenbecks Arch Surg 397:801–807.

Palacios F, Tushir JS, Fujita Y, D'Souza-Schorey C. 2005. Lysosomal targeting of E-cadherin: a unique mechanism for the down-regulation of cell-cell adhesion during epithelial to mesenchymal transitions. Mol Cell Biol 25:389–402.

Peinado H, Olmeda D, Cano A. 2007. Snail, Zeb and bHLH factors in tumour progression: an alliance against the epithelial phenotype. Nat Rev Cancer 7:415–428.

Petrie RJ, Doyle AD, Yamada KM. 2009. Random versus directionally persistent cell migration. Nat Rev Mol Cell Biol 10:538–549.

Rowan AJ, Lamlum H, Ilyas M, Wheeler J, Straub J, Papadopoulou A, Bicknell D, Bodmer WF, Tomlinson IP. 2000. APC mutations in sporadic colorectal tumors: a mutational "hotspot" and interdependence of the "two hits." Proc Natl Acad Sci USA 97:3352–3357.

Sabbah M, Emami S, Redeuilh G, Julien S, Prévost G, Zimber A, Ouelaa R, Bracke M, De Wever O, Gespach C. 2008. Molecular signature and therapeutic perspective of the epithelial-to-mesenchymal transitions in epithelial cancers. Drug Resist Updat 11:123–151.

Sah NK, Khan Z, Khan GJ, Bisen PS. 2006. Structural, functional and therapeutic biology of survivin. Cancer Lett 244:164–171.

Sebag-Montefiore D, Stephens RJ, Steele R, Monson J, Grieve R, Khanna S, Quirke P, Couture J, de Metz C, Myint AS, Bessell E, Griffiths G, Thompson LC, Parmar M. 2009. Preoperative radiotherapy versus selective postoperative chemoradiotherapy in patients with rectal cancer (MRC CR07 and NCIC-CTG C016): a multicentre, randomised trial. Lancet 373:811–820.

Siegel R, DeSantis C, Virgo K, Stein K, Mariotto A, Smith T, Cooper D, Gansler T, Lerro C, Fedewa S, Lin C, Leach C, Cannady RS, Cho H, Scoppa S, Hachey M, Kirch R, Jemal A, Ward E. 2012. Cancer treatment and survivorship statistics, 2012. CA Cancer J Clin 62:220–241.

Stauber RH, Mann W, Knauer SK. 2007. Nuclear and cytoplasmic survivin: molecular mechanism, prognostic, and therapeutic potential. Cancer Res 67:5999–6002.

Thiery JP, Acloque H, Huang RY, Nieto MA. 2009. Epithelial-mesenchymal transitions in development and disease. Cell 139:871–890.

Tojkander S, Gateva G, Schevzov G, Hotulainen P, Naumanen P, Martin C, Gunning PW, Lappalainen P. 2011. A molecular pathway for myosin II recruitment to stress fibers. Curr Biol 21:539–550.

Tsukamoto H, Shibata K, Kajiyama H, Terauchi M, Nawa A, Kikkawa F. 2007. Irradiation-induced epithelial-mesenchymal transition (EMT) related to invasive potential in endometrial carcinoma cells. Gynecol Oncol 107: 500–504.

van den Brink M, Stiggelbout AM, van den Hout WB, Kievit J, Klein Kranenbarg E, Marijnen CA, Nagtegaal ID, Rutten HJ, Wiggers T, van de Velde CJ. 2004. Clinical nature and prognosis of locally recurrent rectal cancer after total mesorectal excision with or without preoperative radiotherapy. J Clin Oncol 22:3958–3964.

Verkaar F, Zaman GJ. 2011. New avenues to target Wnt/β-catenin signaling. Drug Discov Today 16:35–41.

Wei J, Xu G, Wu M, Zhang Y, Li Q, Liu P, Zhu T, Song A, Zhao L, Han Z, Chen G, Wang S, Meng L, Zhou J, Lu Y, Ma D. 2008. Overexpression of vimentin contributes to prostate cancer invasion and metastasis via src regulation. Anticancer Res 28:327–334.

Wong RK, Berry S, Spithoff K, Simunovic M, Chan K, Agboola O, Dingle B, Group GCDS. 2010. Preoperative or postoperative therapy for stage II or III rectal cancer: an updated practice guideline. Clin Oncol (R Coll Radiol) 22:265–271.

Workman P, Al-Lazikani B, Clarke PA. 2013. Genome-based cancer therapeutics: targets, kinase drug resistance and future strategies for precision oncology. Curr Opin Pharmacol 13:486–496.

Wu B, Crampton SP, Hughes CCW. 2007. Wnt signaling induces matrix metalloproteinase expression and regulates T cell transmigration. Immunity 26:227–239.

Yamaguchi H, Condeelis J. 2007. Regulation of the actin cytoskeleton in cancer cell migration and invasion. Biochim Biophys Acta 1773:642–652.

SUPPORTING INFORMATION

Additional supporting information may be found in the online version of this article at the publisher's web-site.